encit 2020

ABCM Associação Brasileira de Engenharia e Ciências Mecânicas

18th Brazilian Congress of Thermal Sciences and Engineering
November 16–20, 2020 (Online)

ENC-2020-0644
THERMAL ANALYSIS OF BRAKE DISCS FOR BAJA SAE VEHICLE

Gustavo Varejão Ferreira Pasqual
Lucival Malcher
University of Brasília, Faculty of Technology, Department of Mechanical Engineering, Campus Darcy Ribeiro, Brasília, Distrito Federal, Brazil
gustavopasqual.enm@gmail.com
lucival.malcher@gmail.com

Abstract. *This paper aims to study the thermal analysis of brake discs applied to a baja SAE prototype in the years of 2019 and 2020 with two different materials, steel SAE 1045 and stainless steel AISI 304. Thus, to analyze the performance of both discs and materials, it was considered 25 braking cycles. As the boundary conditions for the numerical simulations using transient thermal analysis in Ansys, it was applied heat flux in the friction region of pads and disc. It was also applied convection and radiation in the disk body. From the results, it was observed a better heat dissipation of the steel 1045. Finally, the 2019 brake disc was shown to distribute the temperature better when compared to 2020.*

Keywords: *brake disc, thermal analysis, finite element analysis, temperature distribution*

1. INTRODUCTION

The baja SAE program is a proposed challenge for engineering students around the world, in which they have to design, build and race an all-terrain vehicle. The competitions are divided in two stages, static events and dynamics events. One of the dynamics is the four-hour endurance race in which the car is severely tested under the most diverse circumstances. Thus, this work reports a thermal analysis of the brake discs of a baja SAE prototype, Fig. 1.

Figure 1. Baja SAE prototype in the endurance race.

The brake system converts kinetic energy of the vehicle into heat at the friction surface by the heat generation process. Heat generation, and hence, brake temperature, is the product of rubbing velocity between caliper pad and brake disc, mechanical pad pressure, and pad/disc coefficient of friction. Thus, brakes must be designed such that operating temperatures are kept below a certain level to ensure safe and efficient operation of brake components under foreseeable conditions (Limpert, 2011). In a hard braking a large amount of heat flux is generated in a short time and is dissipated through the brake discs, increasing its temperature. After repeated braking, the high temperature of the components can cause brake fade, which is a reduction of the stopping power.

Thus, high temperatures lead to a decrease in the coefficient of friction between pads and disc. For this reason, several researches have been made to characterize this relationship. Recent work (Menezes, 2016) studied the relationship between the friction coefficient of the pads with the contact pressure, temperature and slip speed. Then, he was able to find the fade temperature of the pads. In addition, the temperature increasing of the brake fluid rises its compressibility and can even vaporized it, both increase the pedal travel and this can be linked to a large number of passenger vehicle collisions according to Lee (1999). His work describes a computational model to predict the increase in fluid temperature during

braking. The brake discs are also exposed to high thermal stresses due to high temperature gradients. This can result in large plastic deformations or thermal shocks, that generate macroscopic cracks running through the rotor thickness and along the radius of the brake disc (Mackin *et al.*, 2002).

Therefore, aiming at the continuous optimization of the braking system, numerous researches have been made around the thermal analysis of the brake discs. A mathematical model that is solved analytically to describe the thermal behavior of solid brake discs was made by Talati and Jalalifar (2009), but for complex geometries due to mass reduction or cut patterns, a numerical model must be adopted. The works (Ferranti *et al.*, 2008), (Veloso *et al.*, 2016) and (Vidiya and Singh, 2017) analyze numerically the temperature of the brake discs for formula SAE vehicles and compared them with the experimental results. The studies (Gupta *et al.*, 2017) and (Chavan *et al.*, 2018) analyzed the influence of brake disc cut patterns on the temperature distribution in the discs.

2. METHODOLOGY

In this work, a comparison was made between two front brake discs with different cut patterns used by Piratas do Cerrado team in the years of 2019 and 2020. Thus, in order to analyze the thermal behavior of the discs, some points of interest were selected, Fig. 2. Table 1 shows the properties of each disc. In additional, it was analyzed the influence of two materials with different thermal properties for the manufacture of the discs, steel SAE 1045 and stainless steel AISI 304.

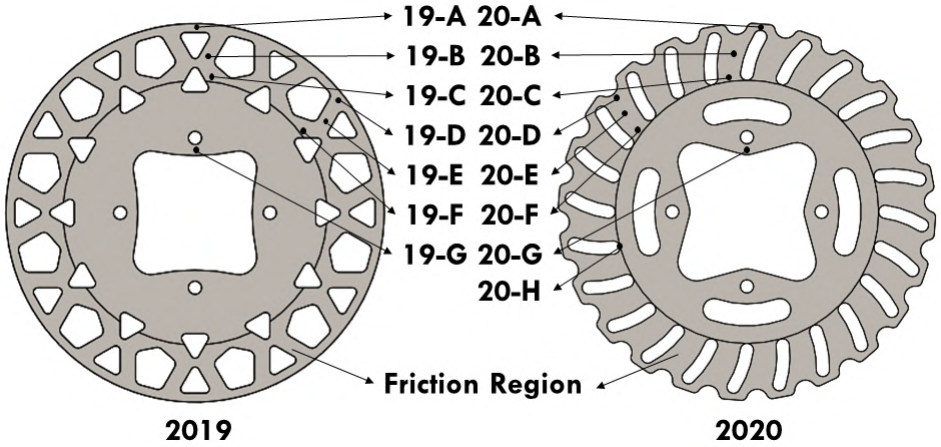

Figure 2. Points of interest of each disc.

Table 1. Discs properties.

Property	2019	2020
Mass (kg)	0.347	0.355
Sweep Area (m^2)	0.014156	0.015376
Thickness (mm)	3.17	3.17
Diameter (mm)	172	172

For the thermal analysis, repeated braking was considered. Thus, the analyzes were performed with 25 braking cycles. Each braking cycle consists of the braking time, in which the heat is generated in the discs, plus the acceleration time, in which the discs are cooled. For braking, it was considered a case of maximum constant deceleration without locking the wheels in an off road ground, which has 0.6 of friction coefficient with the tires. And for acceleration, the experimental speed curve over time was considered to cover 50 meters. Table 2 shows the dynamic performance of the vehicle in a single cycle.

Table 2. Dynamic performance of the baja SAE vehicle.

	Deceleration (m/s^2)	Braking Time (s)	Maximum Speed (m/s)	Acceleration Time (s)
Value	5.52	2.265	12.5	7.735

2.1 Heat generation

During the braking time, it was considered that all kinetic energy of the prototype was converted into thermal energy and absorbed by the brake discs. Then, for a vehicle decelerating on a level surface from a higher velocity V_i to a complete stop, the braking energy E_b is computed by Eq. (1), (Limpert, 2011), where I is the mass moment of inertia of rotating parts, m is the vehicle mass and R is the tire radius. Then, for calculated the braking power and the heat flux in each disc, it was utilized the vehicle properties in Tab. 3.

$$E_b = \frac{m}{2}\left(1 + \frac{I}{R^2 m}\right) V_i^2 \tag{1}$$

Table 3. Vehicle properties.

	Vehicle Mass (kg)	Mass Distribution (%)	Front Components Inertia (kgm^2)	Tire Radius (m)
Value	240	64.29	0.6	0.271

The braking power P_b is equal to braking energy divided by the time during which braking occurs. Considering a constant deceleration, a, the braking power in a single front brake disc is computed by Eq. (2), where I_f is the mass moment of inertia of front rotating parts, Φ is the mass distribution in front axle and t is the braking time. Inspection of Eq. (2) shows that braking power is not constant during the braking process. At beginning of braking, brake power is a maximum, decreasing to zero when the vehicle stops, Fig. 3 (a).

$$P_b = \left(1 + \frac{I_f}{R^2 m\Phi}\right) \frac{m\Phi(V_i - at)}{2} \tag{2}$$

Lastly, the heat flux into which brake disc is equal to braking power divided by the swept area of the discs. Figure 3 (b) shows the heat flux for both discs and it can be observed that the 2019 brake disc has a higher heat flux, because it has an area swept by the pads about 12% smaller than the 2020 brake disc.

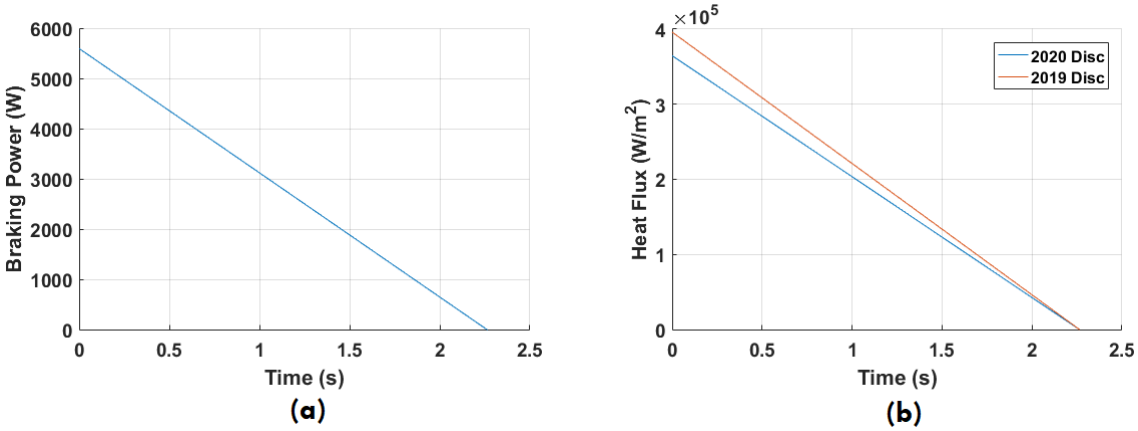

Figure 3. (a) Braking power and (b) heat flux for each disc.

2.2 Heat dissipation

The heat is dissipated through three heat transfer modes: conduction, convection and radiation. However, conduction only redistributes heat, and thus, temperature, and may affect other critical components in an unsafe manner such as bearings, lubricants or seals, (Limpert, 2011).

Textbooks on heat transfer provide a large number of empirical equations for predicting the convective heat transfer coefficient for a variety of test conditions and geometries. But the most of these empirical equations it is applied for passengers cars, which have a different body shape when compared with Baja SAE vehicles, Fig. 1. Thus, the air flow around brake discs is different in passenger cars and Baja SAE. Besides that, progress in the computing capacity and numerical techniques has produced realistic predictions of the air flow around the brake components and the corresponding heat transfer coefficients, (Belhocine and Omar, 2017), (Lee *et al.*, 2018) and (Vidiya and Singh, 2017). For that reason, it was opted to utilized the results obtained by Vidiya and Singh (2017), who, in their work, determined the convection coefficient through a computational fluid dynamics (CFD) analysis for a formula SAE vehicle, which have a body shape

similar to a Baja SAE and they had a good accuracy when compared the numerical temperature of the brake disc surface with the experimental results. Finnved and Nobbelin (2015) have shown that the convection coefficient varies linearly with the car velocity and Fig. 4 (a) shows the results of Vidiya and Singh (2017).

At higher brake temperatures, the radiation cooling capacity of the brakes must be considered. The radiation heat transfer coefficient h_{rad} can be determined by Eq. (3), where σ is the Stefan-Boltzmann constant, ε is the brake disc surface emissivity, T_d is brake disc surface temperature and T_∞ is the ambient temperature. Figure 4 (b) shows the variation of the radiation coefficient with the surface brake disc temperature. It is observed that for hot brakes with the vehicle traveling at low speed, radiation cooling may be the predominant cooling mechanism.

$$h_{rad} = \frac{\sigma\varepsilon(T_d^4 - T_\infty^4)}{T_d - T_\infty} \tag{3}$$

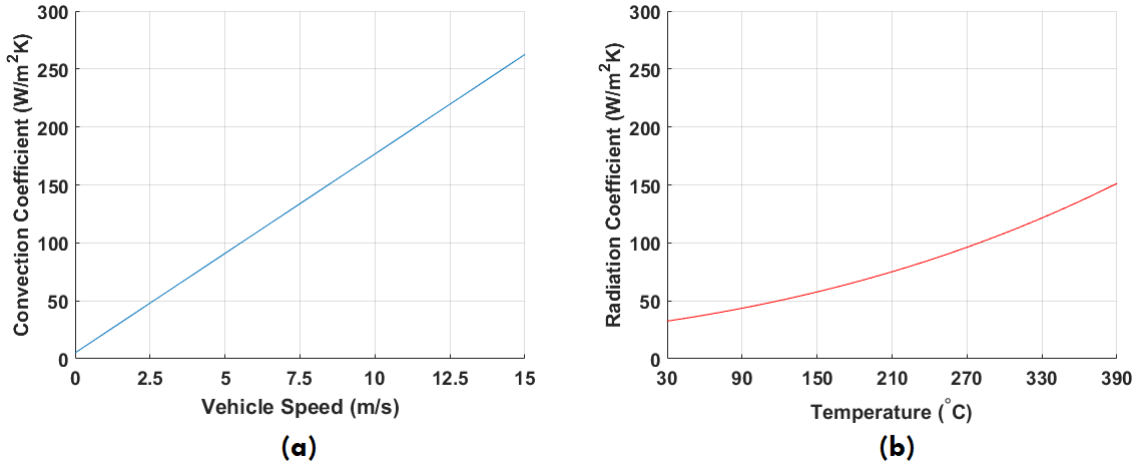

Figure 4. (a) Variation of convection coefficient with velocity and (b) variation of radiation heat transfer coefficient with temperature.

2.3 Boundary conditions

Ansys transient thermal analysis was used to determine the temperature rise of the discs. First, the CAD models were exported to the software and the constants of thermal propriety were informed for each material, Tab. 4. Then, the mesh was generated, using linear tetrahedral elements, Fig. 5. The mesh for 2019 brake disc was generated with 23840 nodes e 82747 elements and for 2020 brake disc was generated with 17681 nodes e 56999 elements.

Table 4. Properties of the materials.

Property	SAE 1045	AISI 304
Specific Heat [J/kg.K]	486	500
thermal conductivity [W/m.K]	50.6	16.2
Density [kg/m^3]	7870	7700
Radiation emissivity	0.5	0.5

As a boundary condition, it was used heat flux, convection and radiation. Thus, the heat flux was applied in the friction region. Then, for convection and radiation all body geometry was selected. The ambient temperature was 30 °C. Table 5 shows the values applied in the boundary condition for each braking cycle, which has 3 steps. The first step is the initial of braking, the second is the end of braking and beginning of the acceleration and the last one is the final of the acceleration. As the transient thermal analysis is time-dependent, the time between the steps from 1 to 2 and 2 to 3 was divided into a few substeps. Thus, a convergence analysis of the results was made for 10, 15, 20 and 25 substeps considering 5 braking cycles. Finally, the analyzes to compare the materials and the geometries were realized with 25 braking cycles.

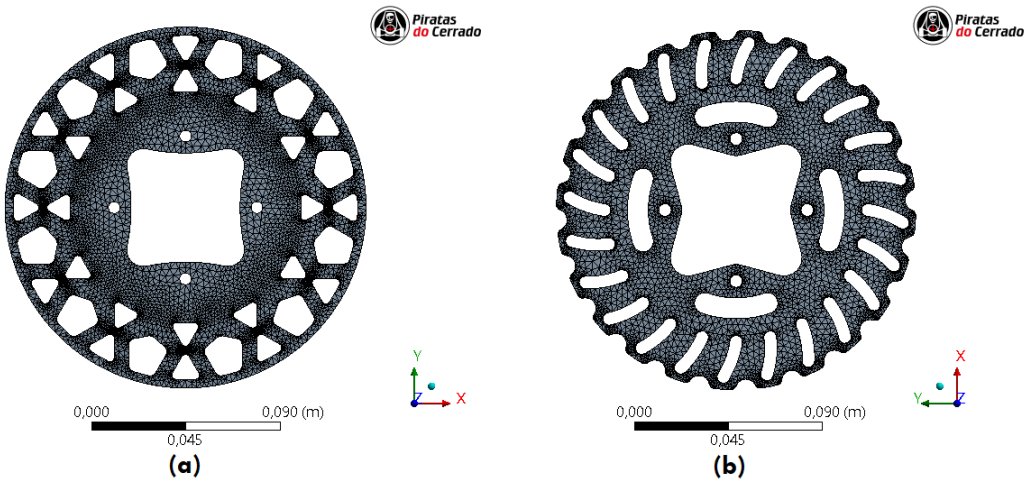

Figure 5. (a) 2019 brake disc mesh and (b) 2020 brake disc mesh.

Table 5. Boundary conditions for one braking cycle.

Step	Time (s)	2019 Heat Flux (W/m^2)	2020 Heat Flux (W/m^2)	Convection Coefficient (W/m^{2}K)
1	0	395814	364400	219.65
2	2.265	0	0	5.15
3	10	0	0	219.65

3. RESULTS AND DISCUSSIONS

3.1 Substeps analysis

The first analysis to be carried out was the convergence of the number of substeps considering 5 braking cycles. For this, it was considered the 2020 brake disc with 1045 as material. Thus, it was observed the convergence of the temperature in the point 20-A and the total heat flux in the point 20-H from 10 to 25 substeps, Fig. 6.

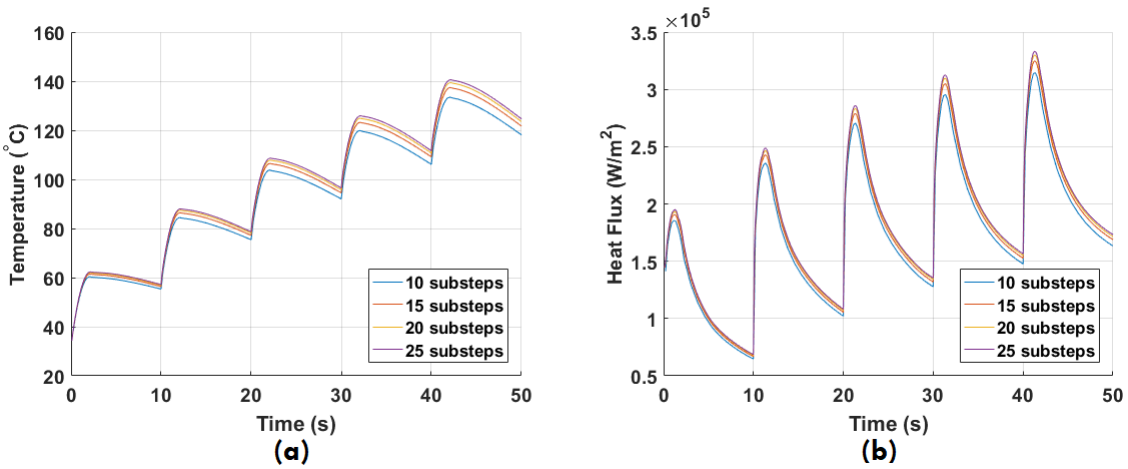

Figure 6. (a) Maximum temperature and (b) maximum heat flux for 2020 brake disc with SAE 1045.

From the results in Fig. 6, it can be observed a relative difference of only 1% greater, when the results of temperature and total heat flux of 25 substeps are compared to 20 substeps. On the other hand, when compared the processing time of the simulation, 25 substeps presented a time 36% bigger. Therefore, for the next analyzes, it was decided to use 20 substeps to decrease the processing time.

3.2 Material analysis

For compare the thermal performance of the materials it was considered 25 braking cycles utilizing the 2020 brake disc. Thus, it was compared the temperature distribution in the disc, Fig. 7, the temperature over time for the points 20-A, 20-F and 20-G, Fig. 8, and the maximum temperature of each point of interest in the friction region, Tab. 6.

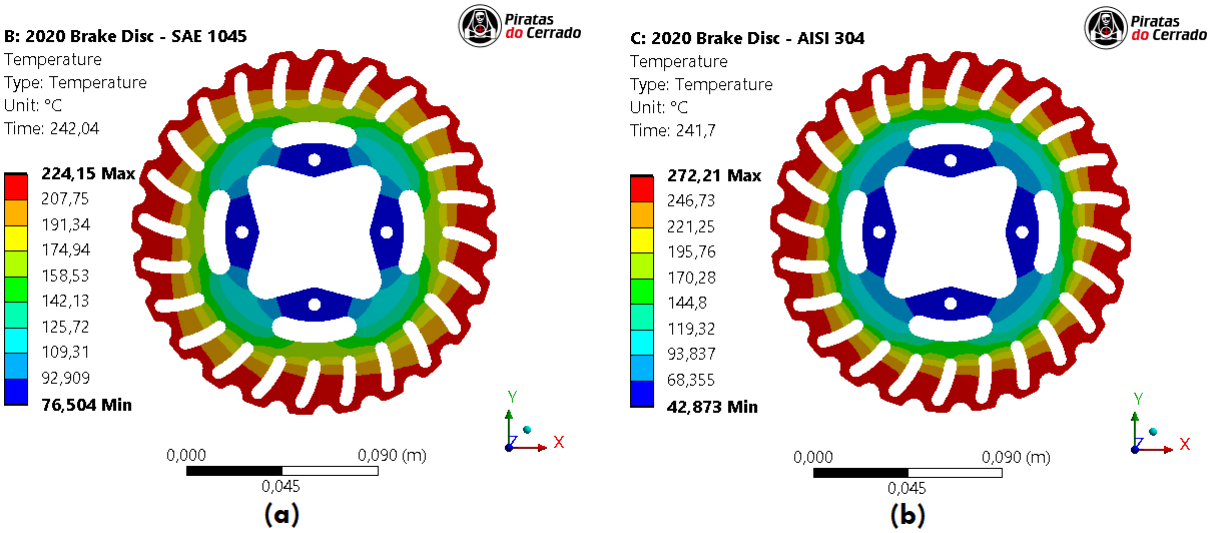

Figure 7. Temperature distribution for (a) SAE 1045 and (b) AISI 304 of 2020 Brake Disc.

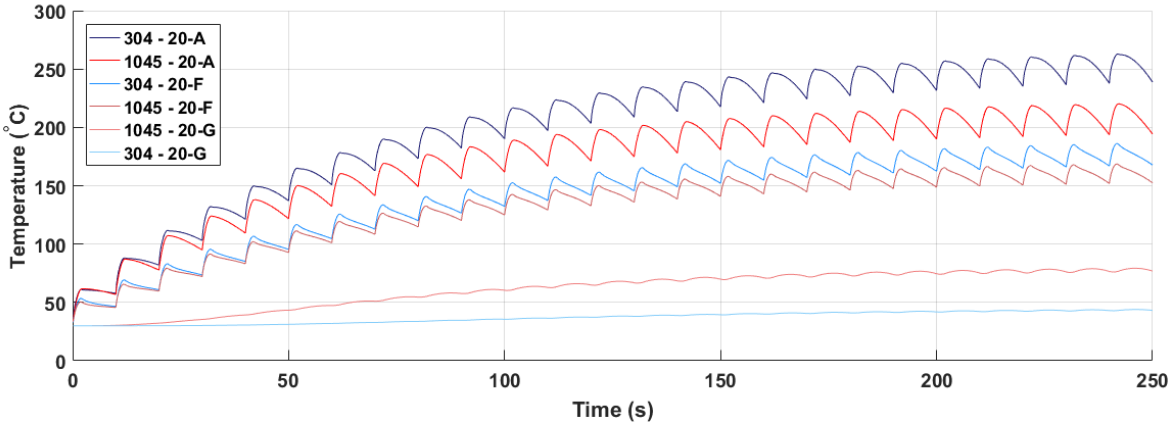

Figure 8. Evolution of temperature in the points of interest for each material.

From the results in Fig.7 and Fig. 8, it can be seen that steel 1045 presents better heat dissipation by conduction, given that for this steel at point 20-A the maximum temperature found was 17.6% lower and at point 20-G 78.4% higher. This can be justified by the fact that the 1045 has a thermal conductivity approximately 3 times greater. In addition, analyzing the points of interest in the friction region, Tab. 6, the average temperature found was 14.2% lower for steel 1045. Finally, it can be observed that there is a tendency to stabilize the maximum temperature reached at each point after 20 braking cycles, this occurs because the heat dissipation by radiation increases with the temperature rise of the disc, then, after repeated braking there is a balance of the heat generated in braking with the heat dissipated in the cooling phase.

Table 6. Maximum temperature in the points of interest for each material.

Material	A (°C)	B (°C)	C (°C)	D (°C)	E (°C)	F (°C)	Average (°C)
304	272	260	189	261	240	175	232
1045	224	218	180	210	200	162	199
Dif. (%)	- 17.6	- 16.2	- 4.8	- 19.5	- 16.7	- 7.4	- 14.2

The brake discs must dissipate the heat in the shortest time possible, decreasing the temperature in the friction region. Because, the friction coefficient of the pads with the disc is a function of the temperature and according to the work of Menezes (2016) the friction coefficient of the same pads currently used by the team has a fade temperature of 200°C. Thus, with stainless steel 304, the temperature would exceed this value. In addition, the heat generated is conducted to the brake fluid, which can cause its vaporization. The team currently uses DOT 4 brake fluid which has a vaporization temperature of 230°C when dry and 155°C when wet. However, it is necessary to perform a thermal analysis with the brake pads and calipers to better predict the temperature that the brake fluid reaches.

3.3 Disc geometry analysis

For compare the brake discs with different geometries it was opted to utilize the SAE 1045 for the material, because it had presented a better performance. Then, the 2019 brake disc was simulated for 25 braking cycles. It can be observed the temperature distribution in Fig. 9. Figure 10 shows the temperature over time for the points A, F and G of each disc. Lastly, the maximum temperature of each point of interest in the friction region can be seen in Tab. 7.

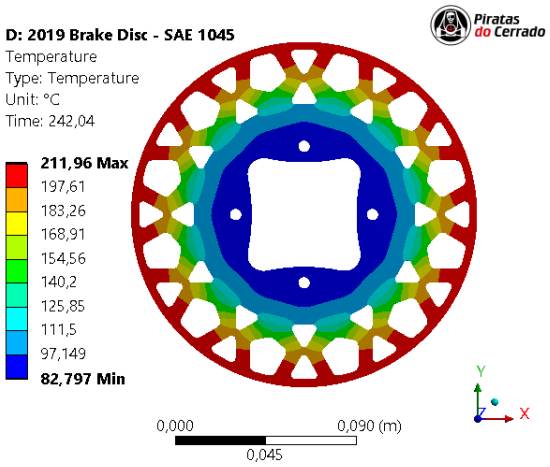

Figure 9. Temperature distribution of 2019 brake disc.

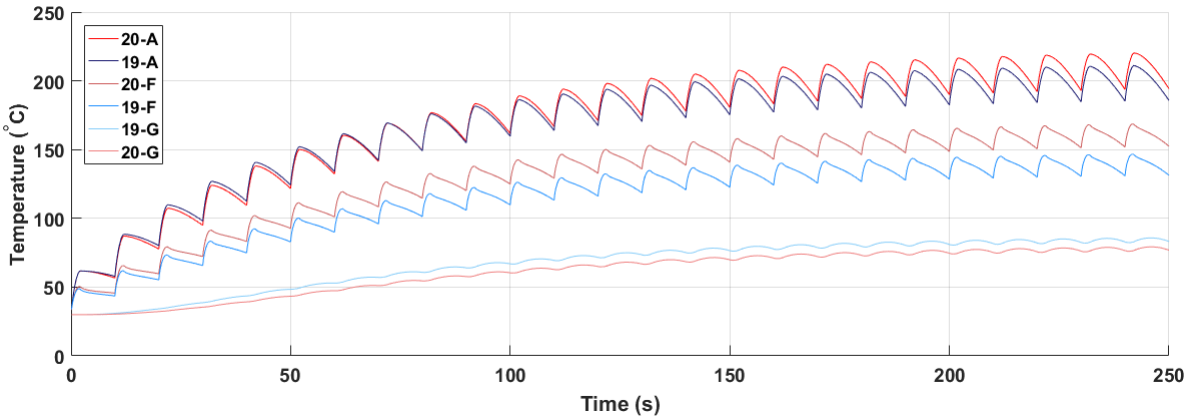

Figure 10. Evolution of temperature in the points of interests for each disc.

From the results it can be seen that the 2019 disc has a better ability to dissipate heat when compared to the 2020 disc, given that the average temperature in the friction region for the 2020 disk is about 6.4% higher, Tab. 7, and the 2019 has a more uniform distribution of temperature along its circumference, Fig. 9. This difference can be explained by the fact that the 2020 disc has 4 cuts to mass reduction in its central region, making heat conduction difficult to the point 20-G, which has a temperature 7.7% higher when compared to the point 19-G.

Table 7. Maximum temperature in the points of interest for each disc.

Brake Disc	A (°C)	B (°C)	C (°C)	D (°C)	E (°C)	F (°C)	Average (°C)
2019	211	190	162	210	189	160	187
2020	224	218	180	210	200	162	199
Dif. (%)	+ 6.2	+ 14.7	+11.1	0	+ 5.82	+ 1.25	+ 6.4

In addition, it can be seen in Fig. 10 that the point that has the largest temperature gradient is the point A, with a maximum temperature difference in the last braking cycle of 12.2% for point 19-A and 13.6% for point 20-A. Therefore, it is believed that these points are critical for the appearance of thermal cracks because they will present the highest amplitudes of thermal stress according to the work (Han *et al.*, 2018). Thus, a detailed coupled thermal-mechanical

analysis must be performed to predict the generation of thermal cracks and consequently to estimate the fatigue life of each disc.

4. CONCLUSION

The thermal performance of the brake discs was predicted through the *Ansys* transient thermal analysis. As a critical condition, it was considered 25 braking cycles. Then, the heat generation in the discs was calculated from the braking power. for heat dissipation, it was considered radiation and forced convection that could be estimated from a CFD analysis. From the results obtained, the best thermal performance was found for the 2019 brake disc with the steel 1045, which was possible to dissipate heat more effectively. Finally, experimental tests must be performed to validate the results obtained in this work, which was unable to performed due to the coronavirus pandemic.

In addition, to complement the thermal study of the brake discs and to understand better the effects of the temperature in the brake system, the following analyzes and tests must be performed in future works:

- Thermal analysis with pads and brake caliper to predict the temperature of the brake fluid;
- Experimental tests of the brake fluid temperature;
- Coupled thermo-structural analysis to predict the generation of thermal cracks and fatigue life of the discs;
- Dynamometer tests to relate the temperature to the friction coefficient of the pads with the disc.

5. ACKNOWLEDGEMENTS

The authors would like to thank the Piratas do Cerrado team for providing the data for this work.

6. REFERENCES

Belhocine, A. and Omar, W.Z.W., 2017. "CFD modeling and computation of convective heat coefficient transfer of automotive disc brake rotors". *Revista Científica*, Vol. 29, No. 2, pp. 116–128.

Chavan, C.B., More, A.S., Patil, N.N. and Baskar, 2018. "Static structural and thermal analysis of brake disc with different cut patterns". *Journal of applied research and technology*, Vol. 16, No. 1, pp. 41–52.

Ferranti, B., Santos, A. and Júnior, A., 2008. "Theoretical and experimental thermal analysis of brake discs for formula sae racing vehicles". *SAE Technical Paper 2008-36-0025*.

Finnved, S. and Nobbelin, S., 2015. *Temperature Estimation in Trailer Disc Brake*. Master's thesis, Lund University, Luden, Sweden.

Gupta, N., Bhandwal, M. and Sikarwar, B., 2017. "Modelling and simulation of brake disc for thermal analysis". *Indian Journal of Science and Technology*, Vol. 10, pp. 1–5.

Han, M., Lee, C., Park, T. and Lee, S., 2018. "Low and high cycle fatigue of automotive brake discs using coupled thermo-mechanical finite element analysis under thermal loading". *Journal of Mechanical Science and Technology*, Vol. 32, No. 12, pp. 5777–5784.

Lee, B.J., Chung, J.T., Jung, Y. and Kim, H., 2018. "Numerical study on fluid flow and heat transfer characteristics of a ventilated brake disc connected to a wheel". *SAE Technical Paper 2008-01-1878*.

Lee, K., 1999. "Numerical prediction of brake fluid temperature rise during braking and heat soaking". *SAE Technical Paper 1999-01-0483*.

Limpert, R., 2011. *Brake Design and Safety*. SAE International, Warrendale, 3rd edition.

Mackin, T.J., Steven, C.N., Ball, K.J., Bedell, B.C., Bim-Merle, D.P., Bingaman, M.C., Bomleny, D.M., Chemlir, G.J., Clayton, D.B., Evans, H.A., Gau, R., Hart, J.L., Karney, J.S., Kiple, B.P., Kaluga, R.C., Kung, P., Law, A.K., Lim, D., Merema, R.C. and Zimmerman, R.S., 2002. "Thermal cracking in disc brakes". *Engineering Failure Analysis*, Vol. 9, No. 1, pp. 63–76.

Menezes, R.C., 2016. *Avaliação da influência da pressão de contato, da velocidade de escorregamento e da temperatura no desgaste e coeficiente de atrito do par pastilha-disco de um mecanismo de freio veicular*. Master's thesis, Universidade Federal de Minas Gerais, Minas Gerais, Brasil.

Talati, F. and Jalalifar, S., 2009. "Analysis of heat conduction in a disk brake system". *Heat and Mass Transfer*, Vol. 45, pp. 1047–1059.

Veloso, W., Garcia, M., Firmino, S., Faria, D. and Assis, J., 2016. "Experimental and numerical thermal analysis of brake disks of a formula sae vehicle". *SAE Technical Paper 2016-36-0457*.

Vidiya, M. and Singh, B., 2017. "Experimental and numerical thermal analysisof formula student racing car disc brake design". *Journal of Engineering Science and Technology Review*, Vol. 10, No. 1, pp. 138–147.

7. RESPONSIBILITY NOTICE

The authors are solely responsible for the printed material included in this paper.